Available online at www.sciencedirect.com
ScienceDirect
International Journal of Rock Mechanics & Mining Sciences 44 (2007) 971–980
International Journal of Rock Mechanics and Mining Sciences
www.elsevier.com/locate/ijrmms

Analysis of coupled gas flow and deformation process with desorption and Klinkenberg effects in coal seams

W.C. Zhu[a], J. Liu[b,*], J.C. Sheng[b], D. Elsworth[c]

[a]School of Resource and Civil Engineering, Northeastern University, Shenyang 110004, China
[b]School of Oil and Gas Engineering, The University of Western Australia, WA 6009, Australia
[c]Department of Energy and Geo-Environmental Engineering, Penn State University, USA

Accepted 11 November 2006
Available online 5 February 2007

Abstract

Coupled gas flow and solid deformation in porous media has received considerable attention because of its importance in pneumatic test analysis, contaminant transport, and gas outbursts during coal mining. Gas flow in porous media is quite different from liquid flow due to the large gas compressibility and pressure-dependent effective permeability. The dependence of gas pressure and gas desorption on gas permeability has a significant effect on gas flow, but has been ignored in most previous studies. Moreover, solid deformation has a direct impact on the porosity, which also leads to desorption or sorption of methane in the coal seam. In this study, a coupled mathematical model for solid deformation and gas flow is proposed and is implemented using a finite element method. The numerical code is used to solve the gas flow equation with Klinkenberg effect, and is validated by comparison with available analytical solutions. Then, it is used to simulate the coupled process during gas migration in a deformable coal seam. The numerical results indicate that the desorption and Klinkenberg effects and mechanical process effect make a significant contribution to gas flow in the coal seam. Without considering the desorption and Klinkenberg effects and the coupling action of mechanical process, the gas pressure in the coal seam would be underestimated.

Keywords: Gas flow; Desorption and Klinkenberg effects; Coupled gas flow and solid deformation; Finite element method

1. Introduction

Coupled gas flow and solid deformation in porous media has received considerable attention because of its importance in areas such as pneumatic test analysis, contaminant transport, and gas outbursts during coal mining [1–3]. One major area of application concerning the coupled gas flow and solid deformation has been considered in the field of petroleum engineering, in which gas flow through porous media is of paramount importance [4]. The transient flow of gas through porous media has also received attention in such field as fluid mechanics, physics, and thermodynamics.

Gas flow in porous media is quite different from liquid flow due to the large gas compressibility and the pressure-dependent effective permeability [5,6]. The dependence of gas permeability on the gas pressure of porous media, which is called the Klinkenberg effect, has a significant effect on gas flow behavior, but it has been ignored in most previous studies. Moreover, the desorption-induced matrix shrinkage also leads to a permeability increase [7]. For methane migration in the coal seam, the porosity decrease due to the compaction of coal also induces the sorption or desorption of methane, which of course changes the gas content. Therefore, it is important to study subsurface gas flow as a coupled process.

Coal-bed gas production is a two-stage process: upon desorption following a reduction in the cleat pressure, gas diffuses out from within the matrix blocks to the cleats; it is then transported along the cleats to the production well. During this process, the geological structures, in situ stresses and high-gas-pressure gradients play important roles in initialing an outburst, with the gas content and

*Corresponding author. Tel.: +61 8 6488 7205.
E-mail address: Jishan@cyllene.uwa.edu.au (J. Liu).

1365-1609/$ - see front matter © 2007 Elsevier Ltd. All rights reserved.
doi:10.1016/j.ijrmms.2006.11.008

gas-pressure gradients being the most dominant factors [8]. Therefore, the gas migration in coal seam is a coupled process in which the gas flow and solid mechanical deformation interact with each other. This process becomes more complex when the gas content, which depends on gas pressure and solid deformation, and the Klinkenberg effect, which reflects the effect of gas pressure on the gas permeability, are included. In previous models, gas migration has been studied as a coupled gas flow and solid deformation process when the gas content is considered to be dependent on gas pressure [8–12]. In the reservoir simulation study of gas-bearing coal beds, the COMET computer model is fully three-dimensional to account for vertical wells intercepting multiple coal seams and structural features [13]. The unique feature of this coupled model is that the stress-induced changes in cleat porosity and permeability, and sorption or desorption of gas, are included. However, these studies do not consider the desorption and Klinkenberg effects for the gas flow analysis, which are also very important for characterizing gas flow in porous media. On the other hand, many other analyses have introduced more complex gas flow equations. For example, Ville [6] took the inertia effect term and the quadratic Forchheimer resistance term into account in the gas flow equations, whereas Wu et al. [1] and Skjetne and Auriault [14] accounted for the pressure-dependent effective permeability effect (Klinkenberg effect). However, due to the complexity of the equation system, they ignored the coupled effect of solid deformation on the porosity, and even the effect on the gas content (sorption or desorption of gas) in the coal seam. Therefore, further efforts should be made in order to fill a gap in the gas migration simulation when the coupling between gas flow and solid deformation, as well as the desorption and Klinkenberg effect of the permeability, are taken into account.

The primary objective of this work is to formulize the fully coupled gas flow and mechanical deformation processes when the desorption and Klinkenberg effects are taken into account. The principal feature of this study is that the dependence of permeability on the gas desorption and gas pressure (desorption and Klinkenberg effects), as well as the coupling between gas flow and solid deformation, are included in the numerical simulations, and their effects on the gas flow are discussed.

2. Governing equations

The present study will involve two coupled processes, gas flow and solid deformation, wherein one physical process affects the initiation and progress of another. The individual processes, in the absence of full consideration of cross couplings, form the basis of well-known disciplines such as elasticity and gas dynamics. Therefore, the inclusion of cross couplings is the key to mathematically formulating the coupled process.

A comprehensive review of mathematical formulations for the coupled thermal, hydraulic, and mechanical (THM) systems can be found in [15]. In this study, we formulate the coupled equations based on [16]. Conservation equations for mass and momentum are derived on the macroscopic scale (all variables are averaged over the REV of the medium) for a saturated, porous elastic medium.

2.1. Mechanical equilibrium equation

The porous medium is assumed to be perfectly elastic so that no plastic deformation occurs. The constitutive relationship of an isotropic linear poroelastic medium can be expressed in terms of the total stress σ_{ij} (positive for tension), strain ε_{ij}, pore fluid pressure change p (negative for suction) as

$$\sigma_{ij} = 2G\varepsilon_{ij} + \frac{2Gv}{1-2v}\varepsilon_{kk}\delta_{ij} - \alpha p\delta_{ij}, \tag{1}$$

in which G is the shear modulus (Pa), v is the Poisson's ratio, δ_{ij} is the Kronecker delta tensor defined as 1 for $i=j$ and 0 for $i\neq j$, and the parameter α ($\leqslant 1$) is the Biot's effective stress coefficient which depends on the compressibility of the rock or coal constituents.

Using compact notation, the equations of equilibrium and the strain-displacement relationship can be expressed as

$$\sigma_{ij,j} + F_i = 0 \tag{2}$$

and

$$\varepsilon_{ij} = \frac{1}{2}(u_{i,j} + u_{j,i}), \tag{3}$$

respectively, where F_i and u_i ($i = x, y, z$) are the component of the net body force and displacement in the i-direction. With the help of Eqs. (1) and (3), a modified Navier equation in terms of displacement under a combination of changes of applied stresses and pore gas pressures can be derived from equilibrium (2) as

$$Gu_{i,jj} + \frac{G}{1-2v}u_{j,ji} - \alpha p_{,i} + F_i = 0. \tag{4}$$

2.2. Gas flow equation

The material is composed of a solid matrix that contains interstitial pore space filled with a freely diffusing pore gas. The absorption or desorption of gas may occur when the gas pressure and porosity of coal seam are changed.

Under isothermal conditions, the gas flow in porous media is governed by a mass balance equation,

$$\frac{\partial m}{\partial t} + \nabla\cdot(\rho_g \mathbf{q}_g) = Q_p, \tag{5}$$

where m is the methane content ($\mathrm{kg\,m^{-3}}$), ρ_g is gas density ($\mathrm{kg\,m^{-3}}$), $\mathbf{q}_g$ is Darcy's velocity of gas phase ($\mathrm{m\,s^{-1}}$), Q_p is source term ($\mathrm{kg\,m^{-3}\,s^{-1}}$), and t is time (s).

The ideal gas law is used to describe the relation between gas density and pressure as

$$\rho_g = \beta p, \tag{6}$$

where ρ_g is gas density ($kg\,m^{-3}$), p is gas pressure (Pa), and β is a compressibility factor ($kg\,m^{-3}\,Pa^{-1}$), defined as

$$\beta = M_g/RT, \tag{7}$$

where M_g is the molecular weight of the gas (kg/kmol), R the universal gas constant ($kJ\,kmol^{-1}\,K^{-1}$), and T the gas temperature (K).

2.2.1. Sorption and desorption of gas from coal seam

The methane content reserved in the rock matrix can be described by the Langmuir's equation [17]:

$$m = \beta\left(\frac{\phi}{p_0} + \frac{a_1 a_2 \rho_s}{1 + a_2 p}\right)p^2, \tag{8}$$

where m is the methane content ($kg\,m^{-3}$), ϕ is porosity, p is gas pressure (Pa), p_0 is unit atmospheric pressure (Pa), which is 1.013×10^5 Pa, ρ_s is the density of coal ($kg\,m^{-3}$), and a_1 and a_2 are Langmuir's constants with units of $m^3\,kg^{-1}$ and Pa^{-1}, respectively. Actually, this equation defines the sorption and desorption of gas from coal seam under changing gas pressure, whereas the sorption isotherm defines the relationship between gas content and pressure only.

The gas flow follows Darcy's flaw, and so Darcy's velocity of the gas phase is defined as

$$\mathbf{q}_g = -\frac{\mathbf{k}_g}{\mu_g}\cdot(\nabla p + \rho_g g \nabla z), \tag{9}$$

where $\mathbf{q}_g$ is Darcy's velocity (m/s), $\mathbf{k}_g$ is gas permeability of rock (m^2), μ_g is gas dynamic viscosity (Pa s), g is acceleration of gravity ($m\,s^{-2}$). In many cases, the gravitational term is relatively small, and $\nabla z = \{0\,0\,1\}^T$ is ignored in later calculations, because the contribution of gas density on the Darcy velocity is relatively small compared to that of the gas pressure.

Substituting Eqs. (6), (8) and (9) into Eq. (5), we find

$$\beta\left[\frac{\phi}{p_0} + \frac{a_1 a_2 \rho_s}{1 + a_2 p} - \frac{a_1 a_2^2 \rho_s}{2(1 + a_2 p)^2}p\right]\frac{\partial p^2}{\partial t} - \nabla\cdot\left(\beta\frac{k_g}{\mu_g}\nabla p^2\right) = Q_p. \tag{10}$$

2.2.2. Desorption and Klinkenberg effects

According to Klinkenberg [18], the effective gas permeability depending on gas pressure is given by

$$k_g = k_\infty\left(1 + \frac{b}{p}\right), \tag{11}$$

where k_∞ is the absolute gas permeability under very large gas pressure at which condition the Klinkenberg effect is negligible (m^2), and b is the Klinkenberg factor (Pa), depending upon the mean free path of the gas molecules which, in turn, depends on pressure, temperature, and molecular weight of the gas. It is generally expected that the Klinkenberg effect is the greatest in fine-grained, low permeability porous media [1]. Jones [19] found that b decreases with increasing permeability and it is fitted to be,

$$b = \alpha_k k_\infty^{-0.36}, \tag{12}$$

where α_k is Klinkenberg effect coefficient ($Pa\,m^{0.72}$), which is fitted to be 0.251 based on the experimental data of 100 cores ranging in permeability from 0.01 to 1000 mD [1]. Other researchers [19,20] also present the similar fitted value of b from a study using approximately 100 low permeability rock samples.

2.2.3. Effect of desorption induced matrix shrinkage

The most important conclusion of the previous work is that desorption of gas causes the coal to shrink [7]. The shrinkage of coal matrix causes the permeability to increase significantly once the pressure falls below the desorption pressure. Above the desorption pressure, the effect of pore volume compressibility is dominant and the permeability decreases. However, once the pressure falls below the desorption pressure, the effect of matrix shrinkage becomes dominant resulting in increased permeability.

According to the fitting excise based on the experimental results of desorption of methane from coal specimen, the variation in permeability with decreasing gas pressure can be expressed with an equation of the form [7]

$$k_{g0} = \frac{c_1}{p} + c_2 + c_3 p^2, \tag{13}$$

where p is the gas pressure, k_{g0} is the permeability at zero stresses, and c_1, c_2, and c_3 are three coefficients that must be determined based on gas desorption experiments. For different experimental conditions, the similar non-linear equations with different coefficients should be given. In the experiments of Harpalani and Schraufnagel [7], $c_1 = 2.25e{-}12$, $c_2 = 7.50e{-}20$, and $c_3 = 4.62573e{-}31$, when the units of pressure and permeability are Pa and m^2, respectively.

Eq. (13) actually describes the influence of both the desorption and Klinkenberg effects on permeability of coal, which is complex and the two effects cannot be separated.

2.3. Cross coupling equation

The effect of gas flow processes on the mechanical process is implicit in Eqs. (1) and (4). In addition, gas content is dependent on the porosity, which is closely related to solid deformation, which is given by [12]

$$\phi = (\phi_0 - \phi_r)\exp(\alpha_\phi \cdot \bar{\sigma}_v) + \phi_r, \tag{14}$$

where ϕ_0 is porosity at zero stress, α_ϕ is stress sensitivity coefficient, which is $5.0 \times 10^{-8}\,Pa^{-1}$ [12], ϕ_r is residual porosity at high stress, and $\bar{\sigma}_v$ is the effective mean stress (with tension positive and in Pa), which is calculated as [12]

$$\bar{\sigma}_v = (\sigma_1 + \sigma_2 + \sigma_3)/3 + \alpha p, \tag{15}$$

where α is Biot's effective stress coefficient [21] and σ_1, σ_2, and σ_3 are first, second, and third principal stresses,

respectively. In the current calculations, we have $\alpha = 1$, which is a reasonable value [12]. Besides, the absolute gas permeability is correlated to the porosity according to the following exponential function [12]

$$k_g = k_{g0} \exp\left[22.2(\phi/\phi_0 - 1)\right], \tag{16}$$

where k_{g0} is the zero stress gas permeability when desorption and Klinkenberg effects are both considered (m^2), and k_g is the gas permeability under non-zero stress condition with desorption and Klinkenberg effects considered.

The above equations (13) and (16) describe three different mechanisms that dominate the permeability changes. The former incorporates the effect of desorption and Klinkenberg effect, while the latter depends on the porosity changes induced by effective stress because the permeability increases with porosity.

In this regard, the permeability at zero stress condition k_{g0} is firstly calculated from Eq. (13) in order to consider the desorption and Klinkenberg effects and, secondly, the permeability at non-zero stress k_g is obtained according to Eq. (16).

It can be seen that the permeability is not only dependent on desorption and Klinkenberg effects, but is also related to the porosity. On the other hand, porosity is related to the effective stress.

2.5. Initial and boundary conditions

For completeness, standard boundary conditions and initial conditions are defined as follows.

2.5.1. Boundary conditions

Stress–displacement conditions for the mechanical analysis are defined as

$$\mathbf{u}(\mathbf{x}, t) = \bar{\mathbf{u}}(\mathbf{x}, t), \quad t \in [0, \infty), \tag{17}$$

$$\sigma(\mathbf{x}, t) \cdot \mathbf{n} = \bar{\mathbf{F}}(\mathbf{x}, t), \quad t \in [0, \infty), \tag{18}$$

where $\bar{\mathbf{u}}(\mathbf{x}, t)$ and $\bar{\mathbf{F}}(\mathbf{x}, t)$ are the known displacement and stress at boundary, respectively, and $\mathbf{n}$ is the outward unit normal vector on the domain boundary.

Fluid flow process:

The Dirichlet condition:

$$p(\mathbf{x}, t) = \bar{p}(\mathbf{x}, t), \quad t \in [0, \infty), \tag{19}$$

The Neumann condition:

$$\frac{\mathbf{k}}{\mu_g} \nabla p \cdot \mathbf{n} = \bar{Q}_l(\mathbf{x}, t), \quad t \in [0, \infty), \tag{20}$$

where $\bar{p}(\mathbf{x}, t)$ and $\bar{Q}_l(\mathbf{x}, t)$ are known boundary gas pressure and gas flux, respectively.

2.5.2. Initial conditions

Initial conditions for the mechanical and gas flow analyses are defined as

$$\mathbf{u}(\mathbf{x}, 0) = \mathbf{u}_0 \ \text{ on } \ V, \tag{21}$$

$$\sigma(\mathbf{x}, 0) = \boldsymbol{\sigma}_0 \ \text{ on } \ V, \tag{22}$$

$$p(\mathbf{x}, 0) = p_0 \ \text{ on } \ V, \tag{23}$$

where $\mathbf{u}_0$, $\boldsymbol{\sigma}_0$, and p_0 are initial values of displacement, stress, and gas pressure at the domain V. The quantity V represents the volume under consideration.

2.6. Numerical implementation in COMSOL multiphysics

The above governing equations, especially the gas flow equation with desorption and Klinkenberg effects, is a non-linear partial differential equation (PDE) with second order for space and first order for time. The non-linearity appears both in space and time domain, and therefore these equations are not possible to be solved analytically. Therefore, the complete set of coupled equations is implemented, and solved by using COMSOL Multiphysics, a powerful PDE-based multiphysics modelling environment [22]. In COMSOL Multiphysics, the specified PDEs may be non-linear and time dependent and act on a 1D, 2D, or 3D geometry. The PDEs and boundary values that are represented by general forms is

$$\begin{cases} d_a \dfrac{\partial u_l}{\partial t} + \nabla \cdot \Gamma_l = F_l, & \text{in } \Omega, \\ -\mathbf{n} \cdot \Gamma_l = G_l + \left(\dfrac{\partial R_m}{\partial u_l}\right)\mu_m, & \text{on } \partial\Omega, \\ 0 = R_m, & \text{on } \partial\Omega. \end{cases} \tag{24}$$

The first equation (24a) is satisfied inside the domain Ω, and the second (24b) (generalized Neumann boundary) and third (24c) (Dirichlet boundary) equations are both satisfied on the boundary of the domain $\partial\Omega$. $\mathbf{n}$ is the outward unit normal and is calculated internally. The equation index l ranges from 1 to N, while the constraint index m ranges from 1 to M. This discussion uses the summation convention. F_l, G_l, and R_m are scalars and can be functions of the space, time, and the solution u_l, whereas Γ_l is a vector and μ_m $(m = 1, 2, \ldots, M)$ are unknown vector-valued functions called the Lagrange multipliers [22]. This multiplier is also calculated internally and will only be used in the case of mixed boundary conditions.

In this study, the independent variable u' denotes three variables, i.e., u, v, and p, which are displacement in x direction, displacement in y direction, and gas pressure, respectively. All the coupling relationships, which are included in those coefficients such as F_l, G_l, R_m and Γ_l, can be given based on friendly input dialogs of COMSOL Multiphysics.

Compared to the loose coupling, in which two sets of equations are solved independently (as in one-way coupling) with two simulators, the fully coupled simulator—COMSOL Multiphysics can solve the coupled multi-physical processes simultaneously. Specifically, we derive a single set of equations incorporating the physics of gas flow and the physics of solid deformation in porous media.

The cross-couplings among multiphysics are defined by the coupled relations between material properties and independent variables.

3. Comparison to the analytical solution

In order to examine the accuracy of the COMSOL Multiphysics in simulating the porous medium gas flow with the Klinkenberg effect, the steady and transient gas flow in rock is numerically solved and compared with the analytical solution. In this regard, it is not possible to find the analytical solution for the coupled gas flow and mechanical process; therefore, the comparison to the analytical solution given only for the gas flow process including the Klinkenberg effect.

3.1. One-dimensional steady gas flow

For the isothermal system (β is a constant), assuming also that porosity ϕ is a constant, under one-dimensional steady-state flow condition, we can simplify Eq. (10) when Eq. (11) is substituted into, and obtain

$$\frac{\partial}{\partial x}\left(\frac{k_\infty \beta (p+b)}{\mu_g}\frac{\partial p}{\partial x}\right)=0. \tag{25}$$

The analytical solution of this equation can be derived under the boundary conditions that are: a constant mass injection rate Q_m at the inlet ($x=0$) and a constant gas pressure $p(L)$ at the outlet ($x=L$). This solution can be written as follows:

$$p(x)=-b+\sqrt{b^2+[p(L)]^2+2b[p(L)]+\frac{2Q_m\mu_g(L-x)}{k_\infty\beta}}. \tag{26}$$

The numerical model of this one-dimensional gas flow problem is carried out for a rock column. The rock column is 10 m long, in which the single-phase gas at isothermal condition is contained. A constant gas mass injection rate is imposed at the inlet of the column, while a constant pressure is kept at the outlet end of the rock column. The parameters, as listed in Table 1, are selected from a laboratory study of the welded tuff at Yucca Mountain [23].

Fig. 1 presents the comparison of pressure along the rock column from our numerical result and the analytical solution, which indicates that the numerical solution of this study is in excellent agreement with the analytical solution for this problem.

In order to discuss the effect of the Klinkenberg effect on the gas flow process, different values of b, which are pertinent to the permeability at high gas pressure as expressed in Eq. (12), are selected and the numerical results are shown in Fig. 2. At the lower permeability (high Klinkenberg factor b), its effect on the gas pressure is very salient. This effect disappears as the permeability at very high gas pressure (k_∞) is increased to $10^{-12}\,m^2$.

Table 1
The parameters used for one-dimensional steady gas flow with Klinkenberg effect

Parameter	Value
Klinkenberg factor, b	7.6×10^5 Pa
Permeability at very high pressure, k_∞	$5.0\times10^{-19}\,m^2$
Length of the column, L	10.0 m
Outlet boundary pressure $p(L)$	1.0×10^5 Pa
Air mass injection rate, Q_m	$1.0\times10^{-6}\,kg\,s^{-1}$
Compressibility factor, β	$1.18\times10^{-5}\,kg\,Pa^{-1}\,m^{-3}$
Porosity, ϕ	0.3
Gas dynamic viscosity, μ_g	1.84×10^{-5} Pa s
Gas density, ρ_g	$1.0\,kg\,m^{-3}$

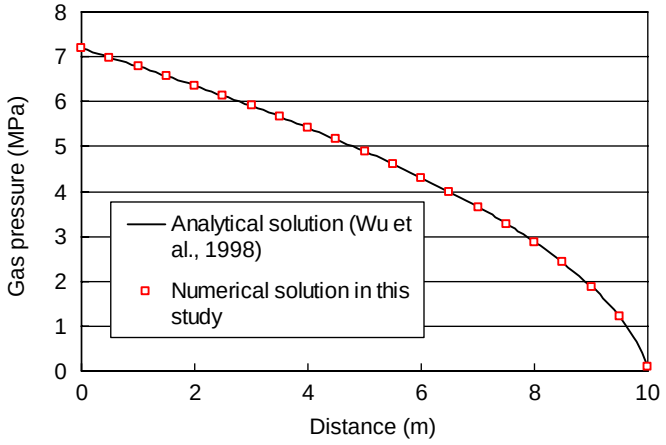

Fig. 1. Comparison of numerical and theoretical results of one-dimensional steady gas flow with Klinkenberg effect.

3.2. Two-dimensional transient gas flow

This is to examine the capability of the COMSOL Multiphysics formulation in simulating transient gas flow with Klinkenberg effect. When no gas desorption is considered and the source term is ignored, the mass balance equation for gas flow is expressed as

$$\frac{\partial \rho_g}{\partial t}+\nabla\cdot(\rho_g q_g)=0, \tag{27}$$

where ρ_g is gas density ($kg\,m^{-3}$), $\mathbf{q}_g$ is Darcy's velocity of gas phase ($m\,s^{-1}$), and t is time (s).

When gravity effects are ignored, substituting Eqs. (6), (9) and (11) into Eq. (27) gives

$$\nabla\cdot(\nabla p_b^2)=\frac{1}{\alpha_p}\frac{\partial p_b^2}{\partial t}, \tag{28}$$

where we use a new variable $p_b=p+b$, α_p is gas diffusivity, which is expressed as

$$\alpha_p=\frac{k_\infty(p+b)}{\phi\mu_g}. \tag{29}$$

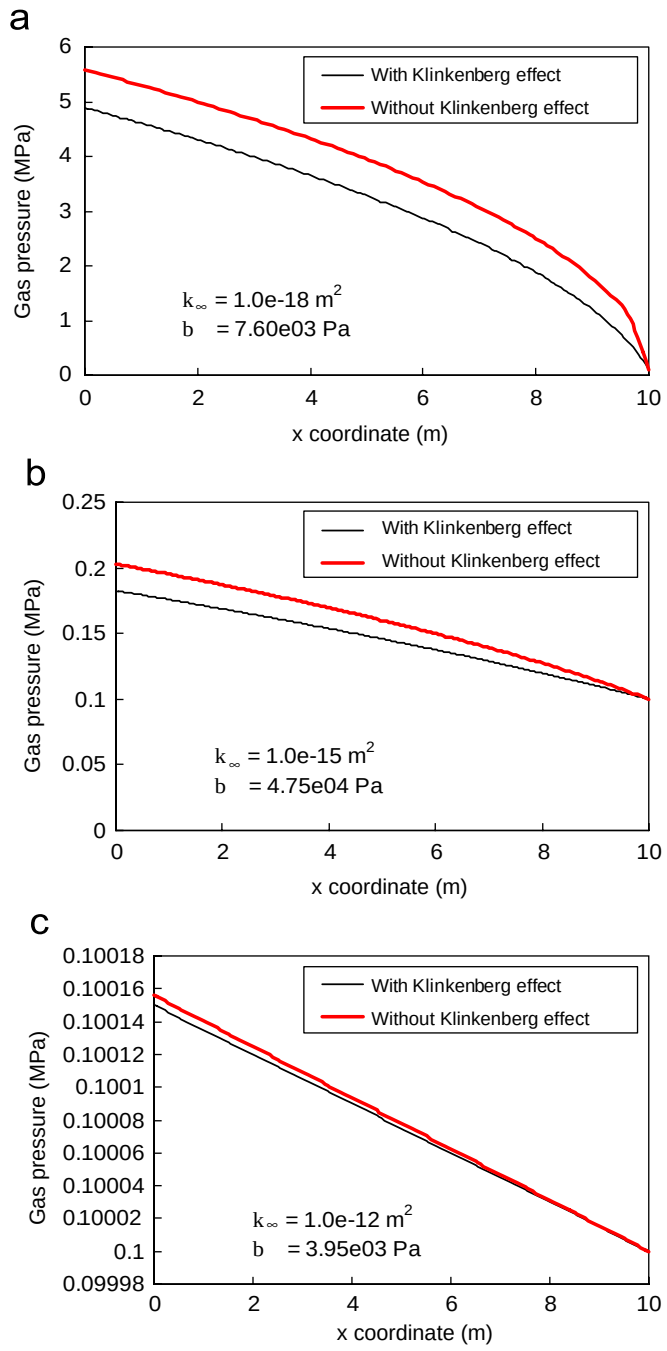

Fig. 2. The gas pressure distribution at different Klinkenberg factors with or without Klinkenberg effect considered.

This example concerns gas injection into a well in a large horizontal, uniform, and isothermal formation, which follows Eq. (28). A constant gas mass injection rate is applied at the well, and the initial pressure is uniform throughout the formation. As listed in Table 2, the parameters that are pertinent to this example are the same as the ones in the analytical solution given by Wu et al. [1].

Fig. 3 presents our numerical result, which is the gas pressure distribution after 10 days of gas injection, in company with the analytical solution and the numerical result calculated with TOUGH2 [1]. It can be found that this numerical solution compares well with the one given by TOUGH2. The analytical solution of Eq. (28) is usually obtained based on linearization of the gas flow equation using the conventional approach [1]. Therefore, the error occurs for the analytical solution when compared with the numerical results given by this study and by TOUGH2.

Table 2
The parameters used for two-dimensional transient gas flow with Klinkenberg effect

Parameter	Value
Klinkenberg factor, b	4.75×10^4 Pa
Permeability at very high pressure, k_∞	1.0×10^{-15} m^2
Air mass injection rate, Q_m	1.0×10^{-6} kg s^{-1}
Porosity, ϕ	0.3
Gas dynamic viscosity, μ_g	1.84×10^{-5} Pa s

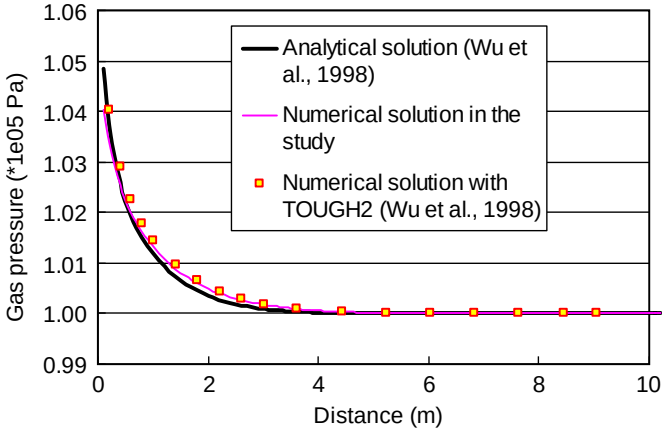

Fig. 3. Comparison of numerical and theoretical results of two-dimensional transient gas flow with Klinkenberg effect (This is the gas pressure distribution after ten days of injection.).

4. Numerical simulation of gas migration in coal seam

In the above section, the validations of the gas flow model and its implementation into COMSOL Multiphysics against theoretical solutions are given when gas flow with Klinkenberg effects is considered. In this section, the coupled model that has been numerically implemented is used to simulate gas migration in coal seam.

In this section, we will focus on simulating the gas migration in coal seam, which is of course dominated by geological structure, in situ stresses, gas content and gas pressure, and not concerned about the real coal or gas outburst because the outburst is, in fact, controlled by failure process of coal.

4.1. Geometry and boundary conditions

The geometry and boundary condition of this example is shown in Fig. 4. The depth from the surface to the top of

the analyzed region is 200 m. The analyzed region is 26 m along the vertical direction and 25 m along the horizontal direction. The coal seam, which is 20 m in length and 6 m in depth, is horizontally layered between two rock layers. The crosscut is 5 m in length throughout all thicknesses of the coal seam. The mechanical deformation is only considered within the rock, while both the coupled gas flow and mechanical deformation analysis are conducted within the coal seam.

For the gas flow process analysis, it is only done in the coal seam. The initial gas pressure in the coal seam is 2.1 Mpa, and a constant atmospheric pressure of 0.101 MPa is applied at the boundary near the working face, while a zero gas flux is applied at the other boundaries. With respect to the solid deformation analysis, the displacements along the vertical direction on the top and bottom boundaries and along the horizontal direction on the left and right boundaries of the analyzed region are fixed. The in situ stress induced by gravity of overburden strata of 200 m height is applied at the top boundary. The initial displacement in the domain is assumed to be zero. The gravity of rock and coal seam is also considered. The coupling relationships, which include the desorption and Klinkenberg effects, as well as the effect of mechanical deformation on porosity and permeability, are implemented into COMSOL Multiphysics and its effect on gas flow is discussed. The desorption and Klinkenberg effects are assumed to have the same properties as that experimented by Harpalani and Schraufnagel [7]. The parameters used in this example are given in Table 3.

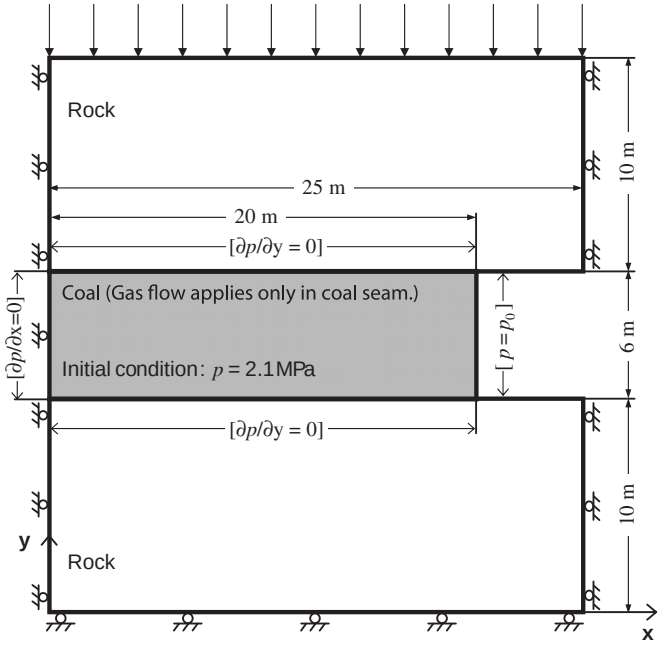

Fig. 4. Geometry and boundary conditions for the coupled mechanical deformation and gas flow process in coal seam, where gas flow applies only in the coal seam. (The equations in the square brackets presented the boundary conditions for gas flow. $p_0 = 1.01e05$ Pa.)

4.2. Gas pressure distribution

Fig. 5 presents the gas pressure distribution at different times. It can be seen that the maximum pressure, which is located at the left boundary, is still the initial gas pressure (2.1 MPa) before time $t = 1e09$ s. The maximum pressures decreases over time, which are 2.1e06, 1.94e06 and 7.35e05 Pa at $t = 1e09$, 1e10 and 1e11 s, respectively. Fig. 6 shows the plot of gas pressure along the horizontal line $y = 13$. For the sake of convenient contrast, the gas pressure distributions when no mechanical process is considered as well as when no mechanical process and no desorption and Klinkenberg effects are considered are also plotted. The desorption effect together with the Klinkenberg effect, leads to the increase of permeability, while the compressive volumetric strain leads to the decrease of permeability. The gas pressure will be underestimated when no coupling of mechanical process is included.

Table 3
The parameters used for transient gas migration in coal seam

Parameter	Value
Young's modulus of rock, E	24500 MPa
Poisson's ratio of rock, v	0.25
Young's modulus of coal, E	7410 MPa
Poisson's ratio of coal, v	0.33
Mass density of coal, ρ_s	1.25×10^3 kg m^{-3}
Klinkenberg factor of coal, b	7.6×10^5 Pa
Stress sensitivity coefficient of coal, α_ϕ	5.0×10^{-8} Pa^{-1}
Zero-stress porosity of coal, ϕ_0	0.083
Residual porosity of coal, ϕ_r	0.02
Langmuir's constant of coal, a_1	3.817×10^{-2} m^3 kg^{-1}
Langmuir's constant of coal, a_2	7.90×10^3 Pa^{-1}
Coefficient for desorption and Klinkenberg effects, c_1	2.25e−12
Coefficient for desorption and Klinkenberg effects, c_2	7.50e−20
Coefficient for desorption and Klinkenberg effects, c_3	4.62573e−31
Compressibility factor of gas, β	1.18×10^{-5} kg Pa^{-1} m^{-3}
Gas dynamic viscosity, μ_g	1.84×10^{-5} Pa s
Gas density, ρ_g	1.0 kg m^{-3}

For the flow process only (without considering the effect of permeability decrease due to compressive volumetric strain), the non-incorporation of desorption and Klinkenberg effects in the numerical analysis underestimates the gas pressure.

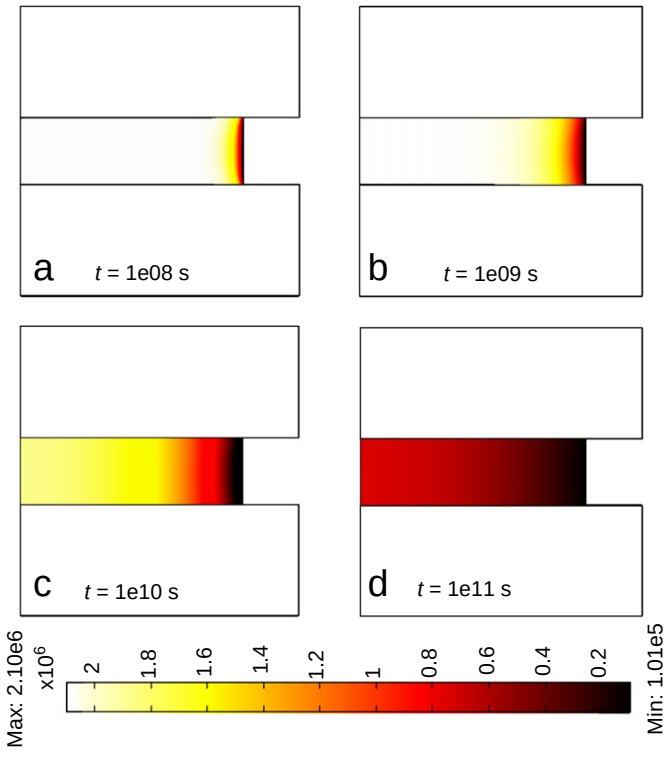

Fig. 5. Gas pressure distribution in the coal seam at different time scales (The maximum pressures are 2.1e06, 2.1e06, 1.94e06, and 7.35e05 Pa at t = 1e08, 1e09, 1e10, and 1e11 s, respectively.).

In this example, the gas in the coal seam is drained gradually, as shown in Fig. 7. Before time t = 1e07 s, the gas content decreases fairly little. Most of the gas drainage occurs from the time t = 1.0e07 and 1.0e11 s. In this respect, ignoring the coupling action of mechanical process leads to fast gas drainage.

4.3. Porosity evolution

Fig. 8 shows the porosity distribution during the gas drainage. The mechanical process is not considered time-dependent. Therefore, the porosity change at different times, as shown in Fig. 8, are only induced by gas pressure variation as the transient gas flow progresses. In general, all the results indicate that the porosity has declined due to the compaction of the coal. In this regard, the decline of the gas pressure increases the effective average compressive stress, thereby restraining the decline of the porosity.

As shown in Fig. 8, although the porosity throughout the coal seam is lower that its initial value at zero stress state ($\phi_0 = 0.083$), the higher porosity is found near the working face. Owing to the Dirichlet boundary of pressure near the working face, there is a fixed porosity that is almost 92% of its zero-stress porosity. The lowest porosity is found at the edges between the working face and roof (or floor), because high compressive stress concentration occurs here. Fig. 9 plots the porosity distribution along the horizontal line that crosses the

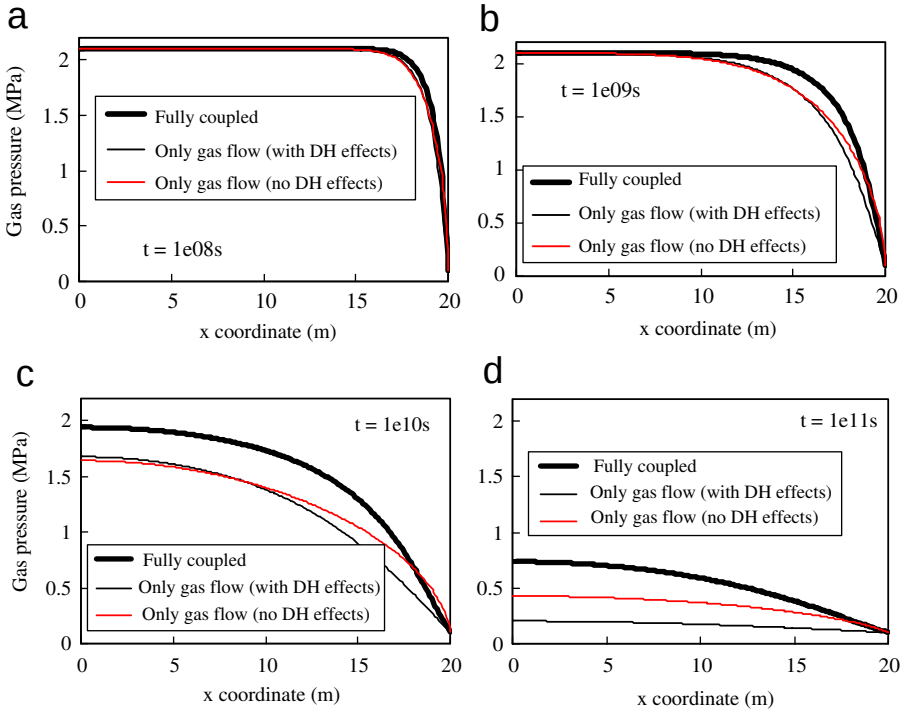

Fig. 6. Gas pressure distribution along the horizontal line y = 13 m for different numerical models, at t = 1e08, 1e09, 1e10, and 1e11 s (Here "DH effects" means the desorption and Klinkenberg effects.).

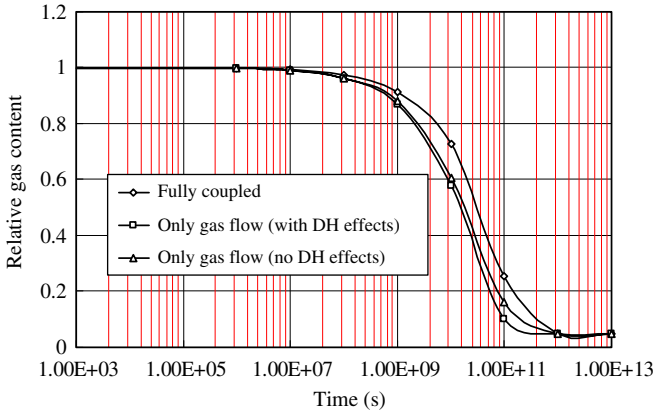

Fig. 7. The gas content in the coal seam at different times (The gas content is obtained when the gas mass at a time is normalized with initial gas mass. Here "DH effects" means the desorption and Klinkenberg effects.).

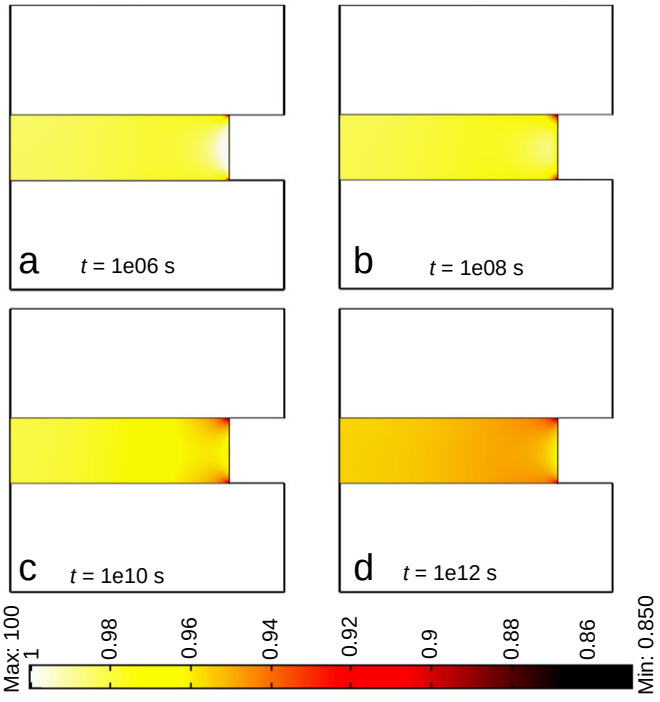

Fig. 8. Porosity evaluation in the coal seam at different time scales during the fully coupled processes.

mid-thickness of the coal seam. With the elapse of time, the ratio of ϕ/ϕ_0 near the left side boundary is decreased gradually from 0.978 at $t = 1e06$ s, to 0.955 at $t = 1e12$ s. The porosity decline owing to the increase of effective compressive stress, is obviously found.

With regard to the major principal stress, it is positive (tensile) only near the work face, and this tensile stress zone becomes smaller over time (Fig. 10). At time $t = 1.0e12$ s, the tensile stress zone disappears, which indicates that the gas flow gradually releases the tensile stress concentration near the working face.

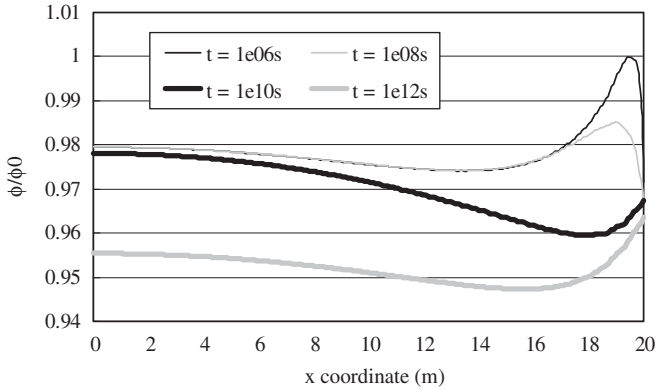

Fig. 9. Porosity distribution along the horizontal line $y = 13$ m at different times during the fully coupled processes. (Here ϕ and ϕ_0 are the porosity under current stress condition and that under zero-stress condition, respectively.)

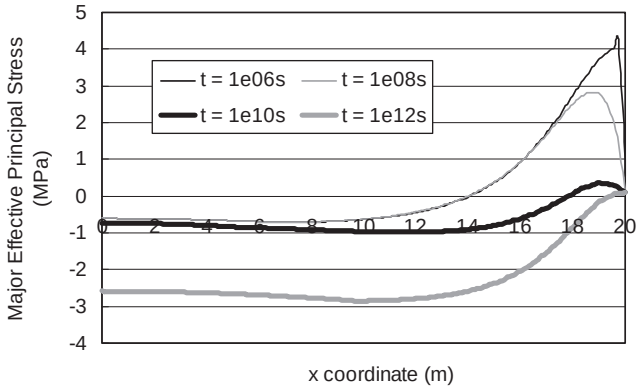

Fig. 10. Major principal stress distribution along the horizontal line $y = 13$ m at different times during the fully coupled processes.

5. Conclusions

In this article, the governing equations for the coupled gas flow and solid deformation in saturated porous media are proposed. In the gas flow equation, the large gas compressibility on permeability, the desorption and Klinkenberg effects on permeability, as well as the sorption and desorption of gas in the coal seam that are related to the gas pressure and coal porosity, are all taken into account. The coupling is achieved when the gas pressure is applied on the solid, and the solid deformation has a significant effect on the porosity of coal. All these governing equations are implemented into COMSOL Multiphysics, a powerful PDE-based multiphysics modelling environment.

The gas flow equation, as well as its implementation in COMSOL Multiphysics, is validated against the analytical solution when the Klinkenberg effect is included. Fully coupled simulation on the gas migration in coal seam is carried and the impact of desorption and Klinkenberg effects, as well as of stress-sensitivity of porosity on the gas pressure distribution, is analyzed, where the gas pressure-dependent methane sorption or desorption is also being considered. The gas pressure will be underestimated when

neither coupling interaction of mechanical process nor the effect of desorption and Klinkenberg is considered. Therefore, in order to capture the gas flow in coal seam effectively, it is very important to consider the desorption and Klinkenberg effects as well as coupling effect of solid deformation during the gas migration.

The numerical simulations in this study have concluded that the porosity will reduce as gas emission; however, the occurrence of in situ rock failure will involve dramatic porosity increase. Therefore, more sophisticated non-linear material failure models will be needed in further work in the future.

Acknowledgments

This work is a result of partial support under grant ARC-DP0209425 and ARC-DP0342446, with additional support provided to the first author by the Natural Science Foundation of China (Grant no.50504005). This support is gratefully acknowledged.

References

[1] Wu YS, Pruess K, Persoff P. Gas flow in porous media with Klinkenberg effects. Transp Porous Media 1998;32:117–37.
[2] Babu DK, Bansal PP. Analytical solution to gas flow through porous media. Paper SPE 39522, SPE/India Oil and Gas Conference and Exhibition, New Delhi, 17–19 February 1998.
[3] Schmidt JG, Westmann RA. Transient gas flow through porous media. Int J Eng Sci 1976;14:19–30.
[4] Clegg MW. The flow of real gases in porous media. Paper SPE 2091, 43rd Ann Fall Mtg Soc Petrol Eng AIME, Houston, September 29–October 2, 1968.
[5] Chan DYC, Hughes BD. Transient gas flow around the boreholes. Transp Porous Media 1993;10:137–52.
[6] Ville AD. On the properties of compressible gas flow in a porous media. Transp Porous Media 1998;22:287–306.
[7] Harpalani S, Schraufnagel RA. Influence of matrix shrinkage and compressibility on gas production from coalbed methane reservoirs. SPE 20729, 65th Ann Tech Conf Exhib, New Orieans, September 23–26, 1990.
[8] Otuonye F, Sheng J. A numerical simulation of gas flow during coal/gas outbursts. Geotech Geol Eng 1994;12:15–34.
[9] Valliappan S, Zhang WH. Numerical modelling of methane gas migration in dry coal seams. Int J Numer Anal Methods Geomech 1996;20:571–93.
[10] Sun PD. Numerical simulations for coupled rock deformation and gas leak flow in parallel coal seams. Geotech Geol Eng 2004;22:1–17.
[11] Zhao YS, Hu YQ, Zhao BH, Yang D. Nonlinear coupled mathematical model for solid deformation and gas seepage in fractured media. Transp Porous Media 2004;55:119–36.
[12] Rutqvist J, Tsang C-F. A study of caprock hydromechanical changes associated with CO_2-injection into a brine formation. Environ Geol 2002;42:296–305.
[13] Young GBC. Computer modelling and simulation of coalbed methane resources. Int J Coal Geol 1998;35:369–79.
[14] Skjetne E, Auriault JL. Homogenization of wall-slip gas flow through porous media. Transp Porous Media 1999;36:293–306.
[15] Jing L, Tsang C-F, Stephansson O. DECOVALEX-An international co-operative research project on mathematical models of coupled THM processes for safety analysis of radioactive waste repositories. Int J Rock Mech Min Sci 1995;32:389–98.
[16] Noorishad J, Tsang C-F. Coupled thermohydroelasticity phenomena in variably saturated fractured porous rocks—Formulation and numerical solution. In: Stephansson O, Jing L, Tsang CF, editors. Coupled thermo-hydro-mechanical processes of fractured media. Amsterdam: Elsevier; 1996. p. 93–134.
[17] Langmuir L. The constitution and fundamental properties of solid and liquids. J Am Chem Soc 1975;36(2):221–95.
[18] Klinkenberg LJ. The permeability of porous media to liquids and gases. In: Drilling and production practice. American Petroleum Institute, 1941. p. 200–13.
[19] Jones FO, Owens WW. A laboratory study of low permeability gas sands. J Pet Tech 1980:1631–40.
[20] Butt SD, Frempong PK, Mukherjee C, Upshall J. Characterization of the permeability and acoustic properties of an outburst-prone sandstone. J Appl Geophys 2005;58:1–12.
[21] Biot MA. General theory of three-dimensional consolidation. J Appl Phys 1941;12:155–64.
[22] COMSOL AB. COMSOL Multiphysics Version 3.2, User's Guide and Reference Guide. Stockholm, 2005.
[23] Reda DC. Slip-flow experiments in welded tuff: the Knudson diffusion problem. In: Tsang C-F, editor. Coupled processes associated with nuclear waste repositories. Am Nucl Soc; 1987. p. 485–93.